

Supporting Information

Electrospray Soft-landing for Construction of Non-covalent Molecular Nanostructures using Charged Droplets at Ambient Condition

Jian Hou, Qingna Zheng, Abraham K. Badu-Tawiah, Caiqiao Xiong, Cuizhong Guan, Suming Chen, Jiyun Wang, Zongxiu Nie, Dong Wang* and Lijun Wan**

Table of Content

Section 1. Materials and Experiment.	3
Materials.....	3
Experimental section	3
Table S1. Molecules used in the experiment and ambient soft-landing parameters.....	4
Section 2. The apparatus of ambient soft-landing.	4
Figure S1. Photograph of the ambient soft-landing set-up.	4
Figure S2. Electric potential simulation of the ion deflector by Simion 8.0.....	5
Scheme S1. The apparatus of a neutral spray or electrospray deposition for surface modification.....	5
Section 3. The assembly of HHTP at the liquid-solid interface.	5
Figure S3. Mass spectrum of HHTP at different conditions.	6
Figure S4. STM image of bare HOPG surface.....	6
Figure S5. STM image of 2,3,6,7,10,11-hexahydroxy-triphenylene (HHTP) on HOPG prepared by drop-casting method.....	7
Table S2. Landing current by spraying HHTP solutions at different concentrations.	7
Figure S6. STM images of HHTP on HOPG prepared by neutral spray.	8
Figure S7. Carbon 1s and Oxygen 1s XPS photoelectron peaks for HHTP on the HOPG	8
Figure S8. STM image of HHTP patterns soft-landed at 2kV.	9
Figure S9. Mass spectrum of 2,3,6,7,10,11-hexahydroxy-triphenylene (HHTP) in methanol by electrospray ionization with 80°C heated drying tube ahead of mass spectrometer.	9
Figure S10. Relative positions of HHTP patterns after landing.....	10
Section 4. Simulation of HHTP interactions by DFT.	10
Figure S11. Optimized geometries of HHTP and HHTP+H ⁺	11
Section 5. Analysis the deposited substances by ambient soft-landing	11
Figure S12. Mass spectra of substances before and after soft-landing process.....	12
Figure S13. High resolution X-ray photoelectron spectra recorded for C ₁₈ H ₃₇ NH ₂	12
Figure S14. Relative positions of n-octadecylamine patterns after soft landing.....	13
Section 6. The assembly of mixed n-octadecylamine and n-octadecanoic acid.....	14
Figure S15. Results of mixed n-octadecylamine and n-octadecanoic acid.....	14
References	14

Section 1. Materials and Experiment.

Materials

n-octadecylamine ($\text{CH}_3(\text{CH}_2)_{17}\text{NH}_2$), n-octadecanoic acid ($\text{CH}_3(\text{CH}_2)_{16}\text{COOH}$), 10,12-pentacosadiynoic acid (PCDA $\text{CH}_3(\text{CH}_2)_{10}\text{C}\equiv\text{C}-\text{C}\equiv(\text{CH}_2)_9\text{COOH}$), 1,3,5-Benzenetribenzoic Acid (BTB $\text{C}_{27}\text{H}_{18}\text{O}_6$) and 2,3,6,7,10,11-hexahydroxy-triphenylene (HHTP $\text{C}_{18}\text{H}_{12}\text{O}_6$) bought from Sigma Aldrich were used without further purification. Methanol and tetrahydrofuran of HPLC grade were from Fisher Chemical. Water used in the experiment was purified by a Milli-Q water purification system (Millipore, Milford, MA).

Experimental section

Nanostructures created by ambient soft-landing. To form self-assembled monolayers of molecules by ambient soft-landing, n-octadecylamine, n-octadecanoic acid, 10,12-pentacosadiynoic acid (PCDA) and 2,3,6,7,10,11-hexahydroxy-triphenylene (HHTP) were dissolved in methanol. 1,3,5-Benzenetribenzoic Acid (BTB) was dissolved by a methanol and THF solution (volume ratio 1/1). For electrospray, the nitrogen nebulizer gas pressure was maintained between 20 and 30 psi. A high DC voltage potential of 5 kV was applied to the electrospray emitter through the metal tip of 500 mL Hamilton syringe. The flow rate of the syringe pump was 2 $\mu\text{L}/\text{min}$. The top two deflecting electrodes on the right side are grounded and the landing/deflecting voltage of 5 kV was applied onto the bottom electrode; the polarity of this landing voltage was opposite to that of the ESI spray voltage. (Figure 1) The drying tube is also grounded to allow the ions fly through at room temperature. The components in the methanolic solution were ionized and deposited onto a freshly cleaned HOPG (quality ZYB, Digital Instruments, Santa Barbara, CA) surface. The HOPG surfaces were cleaned by mechanical exfoliation with tapes before soft-landing. Electrospray generates a continuous beam of ions for the entire duration (60 min) of the experiment. After 1 hour of soft-landing, the area of the HOPG surface on which ions had impinged was imaged by scanning tunnel microscopy. Specific conditions of each molecules were listed in Table S1. To measure the landing current, we let the landed ions hit onto a copper plate instead of HOPG. The copper plate is connected to an ammeter which is composed of a current amplifier and an oscilloscope.

To characterize and confirm the identity of the soft-landed species, the landed species were collected by washing the surface using 8 μL methanol/water (1:1, vol./vol.) solution. Ions collected from the soft-landing of 1,3,5-benzenetribenzoic acid (BTB) were washed into 8 μL methanol/THF/water (1:2:1, vol/vol) solution. The resulting analyte solutions were analyzed by nanospray ionization mass spectrometry performed on Thermo LTQ mass spectrometer (Thermo Fisher, San Jose, Calif., USA). A mixture of n-octadecylamine and n-octadecanoic acid solution (1 mmol/L in methanolic solution) was also soft-landed. In all experiments, an ESI spray voltage of +5 kV or -5 kV was used for the creation of charged droplets, which were subsequently deflected and focused onto the HOPG on which assemblies were created.

STM experiment. The STM experiments were conducted with a Nanoscope IIIa SPM (Digital Instruments, Santa Barbara, CA) in air at room temperature. Mechanically cut Pt/Ir tips (90%/10%) were used as probes, which were conditioned by short voltage pulses when needed. All images were recorded using constant current mode and shown without further processing except plane subtractions to remove the tilting effect of the substrate plane. The specific tunneling conditions are given in the figure captions.

Calculation. Density functional theory (DFT) calculations using Gaussian 09²⁸ program are performed for the structures of $\text{C}_{18}\text{H}_{12}\text{O}_6$ (HHTP) and $\text{C}_{18}\text{H}_{13}\text{O}_6^+$ (HHTP+ H^+) and the interaction of $\text{C}_{18}\text{H}_{12}\text{O}_6 \cdots \text{C}_{18}\text{H}_{12}\text{O}_6$,

$C_{18}H_{13}O_6^+ \dots C_{18}H_{13}O_6^+$ and $C_{18}H_{13}O_6^+ \dots C_{18}H_{13}O_6$ systems. The hybrid B3LYP functional^{29,30} in combination with 6-311+G(d) basis set³¹ are used. The calculated energies reported herein are with zero-point vibrational energy correction (ΔH_{0K}).

Table S1. Molecules used in the experiment and ambient soft-landing parameters.

Name	Formula	Molecular Weight	Concentration	Landing current	Deposition Time
triphenylene-2,3,6,7,10,11-hexaol (HHTP)	C18H12O6	324.29	0.5 mmol/L	600pA	1h
n-octadecylamine	C18H39N	269.52	5 mmol/L	600pA	1h
n-octadecanoic acid	C18H36O2	284.48	5 mmol/L	600pA	1h
10,12-pentacosadiynoic acid (PCDA)	C25H42O2	374.61	0.5 mmol/L	600pA	1h
1,3,5-Benzenetribenzoic Acid (BTB)	C27H18O6	438.43	5 mmol/L	600pA	1h

Section 2. The apparatus of ambient soft-landing.

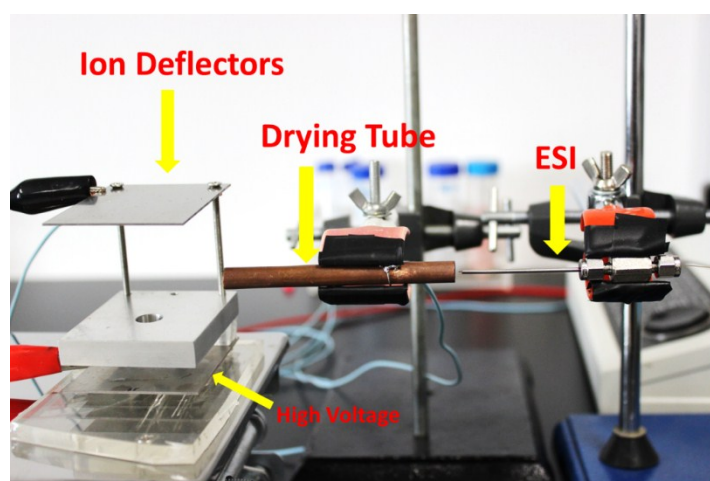


Figure S1. Photograph of the ambient soft-landing set-up. The ambient SL set-up used in the experiment is constituted of three part: i) the electro spray produces charged droplets; ii) solvent of droplets evaporates when flying through the drying tube; iii) dehydrated ions land on the substrate in a vertical high DC field. In the ambient soft-landing apparatus, the electric field between the middle electrode plate and the bottom electrode plate has a great impact on the landing efficiency. Fixing the distance between top plate and middle plate at 4 cm, we simulate the electric potentials when altering the distance between the middle and bottom electrode plate and the high voltage put on the bottom electrode plate by software Simion 8.0.

Supporting Information

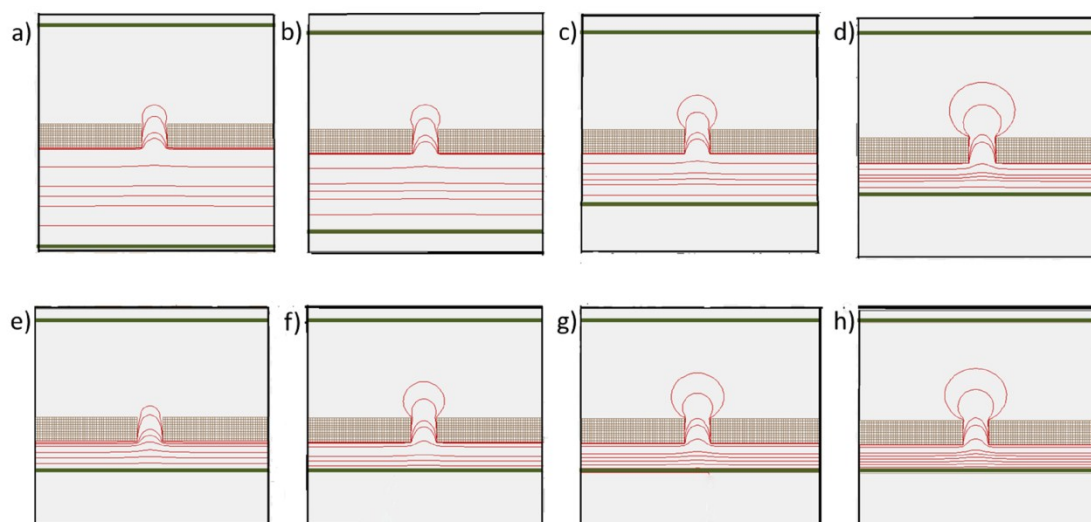
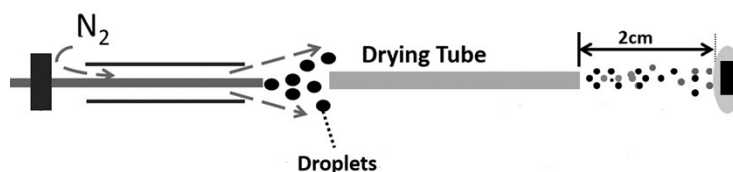


Figure S2. Electric potential simulation of the ion deflector by Simion 8.0 (cross section view). The distance between the middle electrode and bottom electrode was at a) 4 cm, b) 3 cm, c) 2 cm and d) 1 cm when the voltage is 5kV on the bottom electrode. e) 2kV, f) 3kV, g) 4kV, h) 5kV voltage on the bottom electrode is simulated under the same distance of 1 cm, respectively. We set the distance as 1 cm and 5kV voltage in the experiment. Higher electric field was not used to prevent discharge phenomena at the ambient conditions. The green lines represent the top electrode and the bottom electrode. The middle electrode is shown in grid. The red lines are isopotential lines.



Scheme S1. The apparatus of a neutral spray or electro spray deposition for surface modification. In the neutral spray experiment, the set-up was similar to soft-landing, only that the deflecting electrodes were removed and no high voltage on ESI. HOPG was put just at the center of deflecting electrodes. In the electro spray deposition, a 5kV voltage was applied on the spray.

Section 3. The assembly of HHTP at the liquid-solid interface.

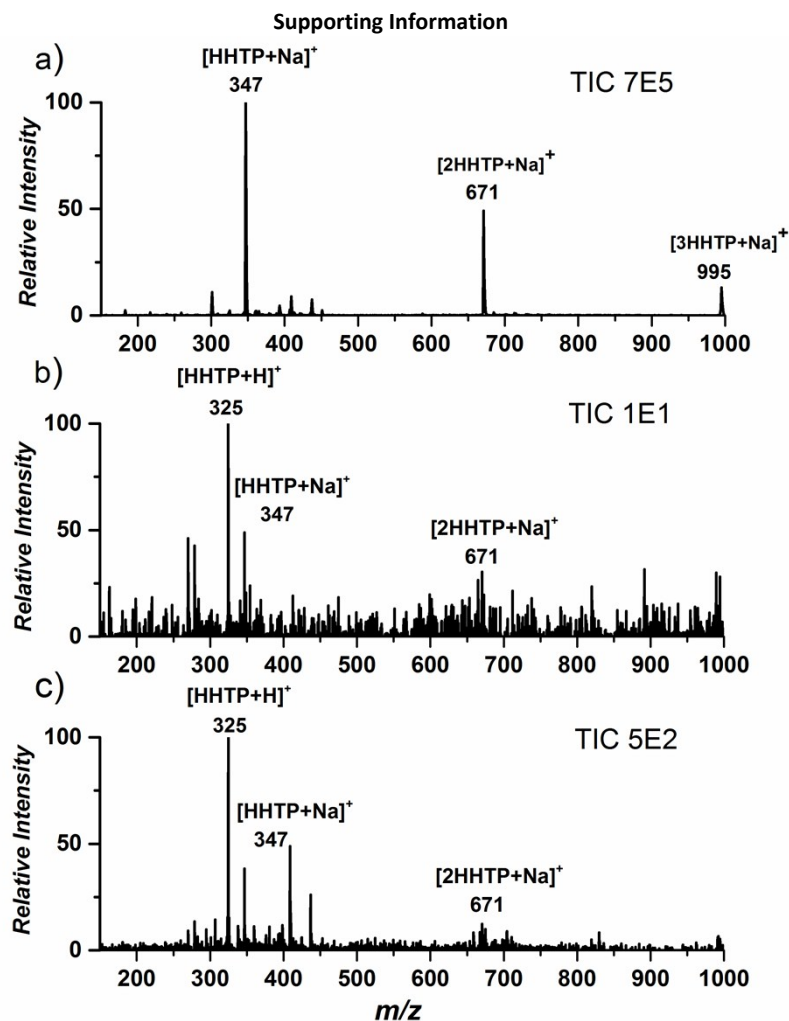


Figure S3. Mass spectrum of HHTP at different conditions. a) Mass spectrum of HHTP collected by inserting the drying tube between the ESI ion source and the mass spectrometer. Ion yield is lower than direct ESI, but the species are identical. HHTP are prone to form multimer, even in the gas-phase. b) mass spectrum of $[HHTP-H]^-$ ions generated by ESI in the negative mode; c) mass spectrum of soft-landed HHTP washed off from silica substrate with methanol and H_2O (1:1). $[HHTP+H]^+$ formed is because H_2O is a proton donor; d) the MS/MS of $[HHTP+Na]^+$ analysed by ESI. It confirms that little fragment were observed in the washed HHTP mass spectrum.

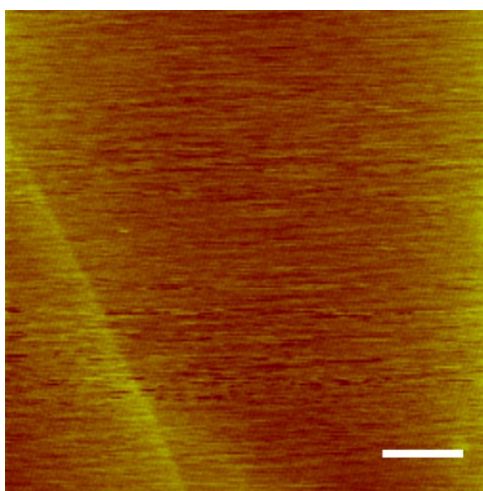


Figure S4. STM image of bare HOPG surface (scale bar 50nm).

Supporting Information

THF is one of the most commonly used solvent in liquid-solid interface assembly because of its good solubility and spreadability. The assemblies below were prepared by deposition of 2.5 μL HHTP in THF onto a freshly cleaned HOPG. As methanol was used as solvent in SL, we also deposit HHTP in methanol on HOPG to exclude solvent effect. These two kinds of solvent both leads to HHTP clusters on HOPG.

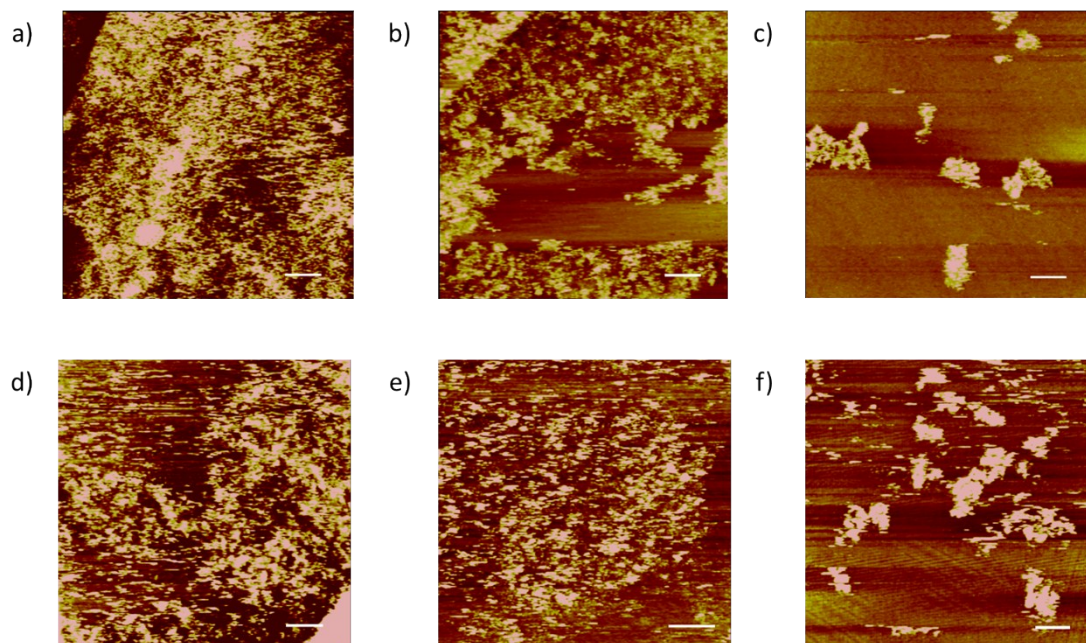


Figure S5. STM image of 2,3,6,7,10,11-hexahydroxy-triphenylene (HHTP) on HOPG prepared by drop-casting method. 2.5 μL HHTP solution were casted at a concentration of a) 10^{-4}mol/L , b) 10^{-5}mol/L , c) 10^{-6}mol/L in THF and d) 10^{-4}mol/L , e) 10^{-5}mol/L , f) 10^{-6}mol/L in methanol on HOPG. The molecules clusterize on the THF-HOPG interface or methanol-HOPG interface. Image conditions: a) $I_t = 500\text{pA}$; $V_{\text{bias}} = 700\text{mV}$. b) $I_t = 450\text{pA}$; $V_{\text{bias}} = 847\text{mV}$. c) $I_t = 450\text{pA}$; $V_{\text{bias}} = 847\text{mV}$. d), e) f), $I_t = 500\text{pA}$; $V_{\text{bias}} = 700\text{mV}$. The scale bar is 12.5nm.

Table S2. Landing current by spraying HHTP solutions at different concentrations.

Sprayed concentration	solution	Landing current
5mmol/L		1nA
0.5mmol/L		600pA
0.05mmol/L		400pA

We observe that the landing currents of HHTP at different initial concentrations are different. The results and corresponding concentration are listed in Table R1. Thus, by adjusting the concentration used in electro spray, landing current can be controlled. As the landing current is closely related to the coverage of landed species, we would like to use the same landing current for these different molecules to obtain a similar coverage. It should be pointed out that because of the precision of the method to measure the landing current, the landing currents of the HHTP, octadecylamine, octadecanoic acid, PCDA and BTB are not precisely the same of 600pA.

Supporting Information

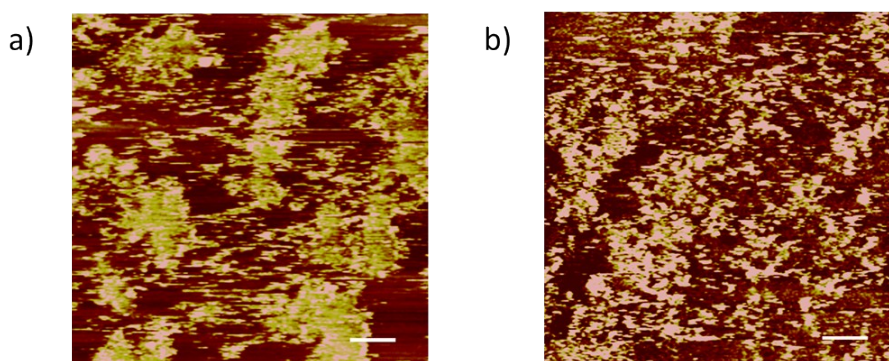


Figure S6. STM images of HHTP on HOPG prepared by neutral spray. HHTP of 10^{-4} mol/L in methanol a) and THF b) was sprayed for 15min, respectively. For high active molecules like HHTP, we assume an ionic process for its assembly is necessary. Image conditions: a) $I_t = 500\text{pA}$; $V_{\text{bias}} = 700\text{mV}$. b) $I_t = 405\text{pA}$; $V_{\text{bias}} = 770\text{mV}$. Scale bar is 10nm.

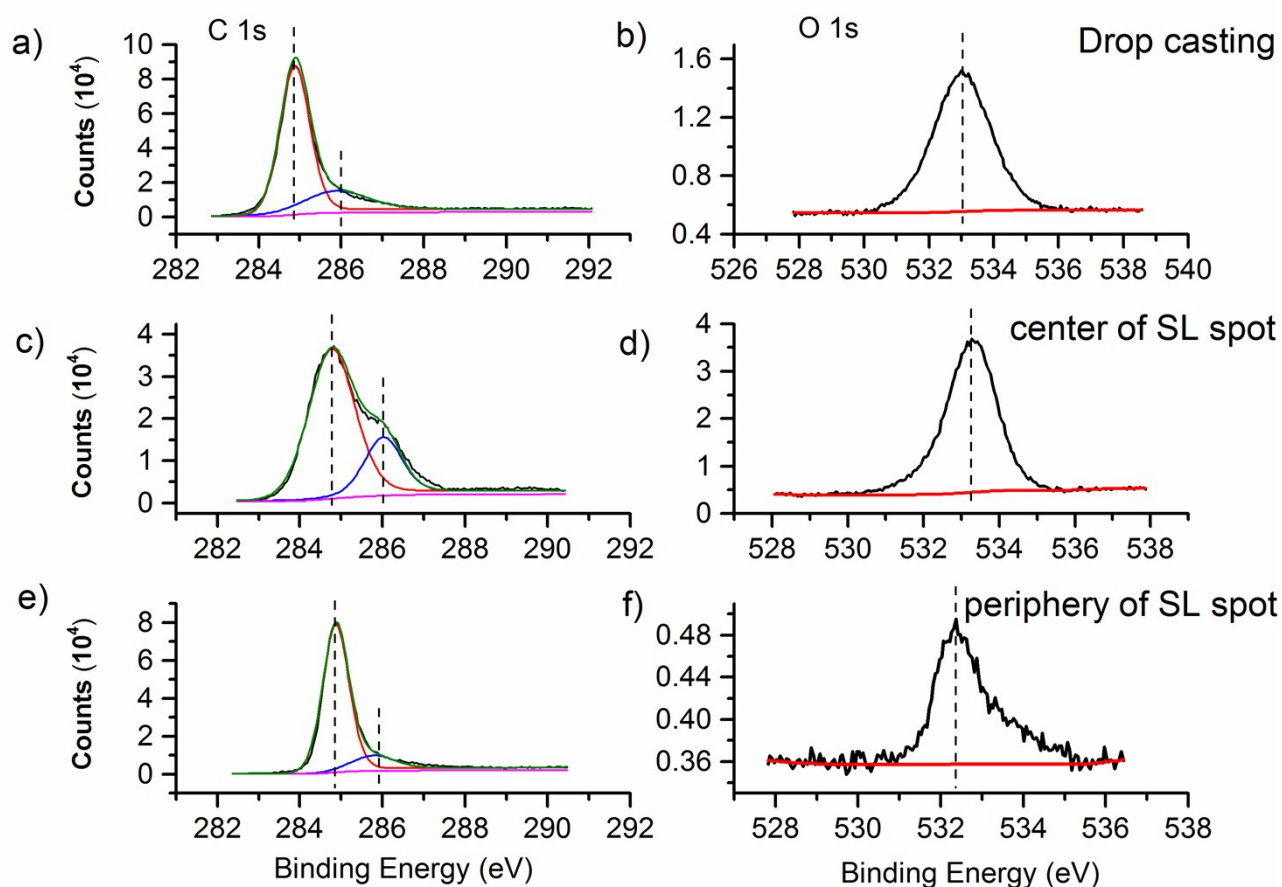


Figure S7. Carbon 1s and Oxygen 1s XPS photoelectron peaks for HHTP on the HOPG prepared by drop-casting method and SL method. a) and b) are recorded by drop-casting method, c) and d) are recorded at the center of SL spot, e) and f) are at the periphery of SL spot. The energies are 284.8 eV and 285.9 eV for C 1s in all three samples. O 1s appear at 533.0 eV for b) and d), but shifts to 532.0 eV at the surrounding of landing spot, presenting O^- property at the periphery domain of landing spot.

Supporting Information

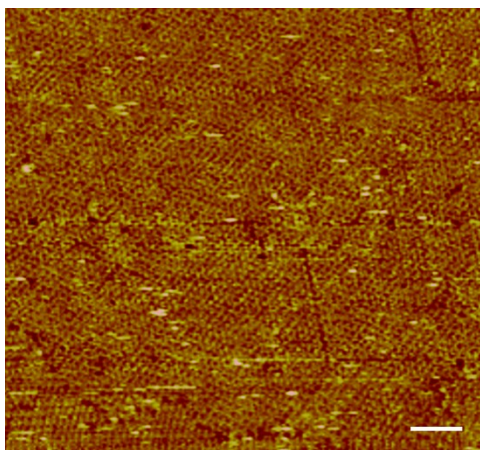


Figure S8. STM image of HHTP patterns soft-landed at 2kV. Image condition: $V_{\text{bias}} = 732 \text{ mV}$, $I_t = 513 \text{ pA}$. The scale bar is 10nm.

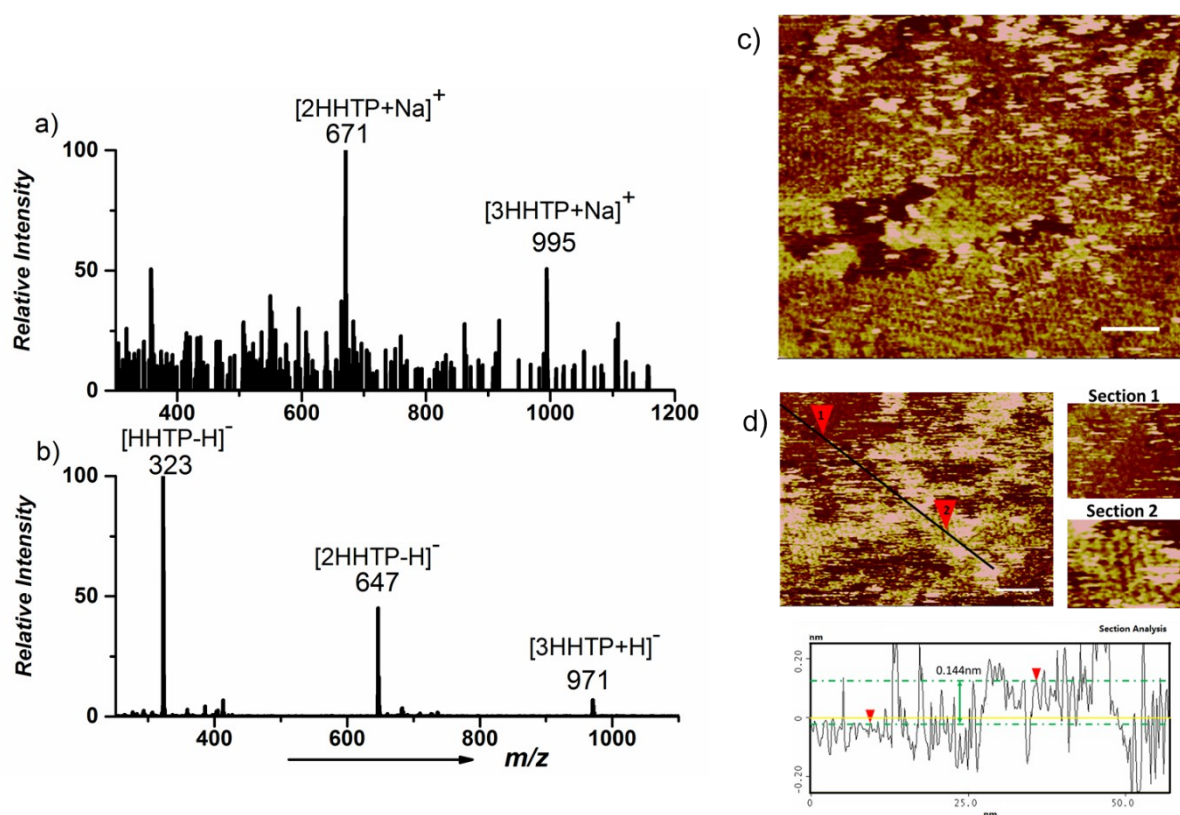


Figure S9. Mass spectrum of 2,3,6,7,10,11-hexahydroxy-triphenylene (HHTP) in methanol by electro spray ionization with 80°C heated drying tube ahead of mass spectrometer. a) In positive ion mode, $[2M+Na]^+$ with trimmers are observed. b) In negative mode, $[M-H]^-$, $[2M-H]^-$ and $[3M-H]^-$ dominate the mass spectrum. c) STM image of HHTP on HOPG prepared by positive electro spray soft-landing with the drying tube heated to 80 °C. The formed close packing of HHTP were consistent with that at room temperature. d) STM image of multilayered HHTP on HOPG constructed by negative electro spray soft-landing. The red triangle indicated two sections from different layers on the surface. The amplified images are on the right. Section 1 is a single layer of HHTP assembly and section 2 is the second or third layer. The vertical distance between the two layers is 0.144nm, which could be one or two atom layer. The brightest section in the image are higher layers. Image Condition: c) $I_t = 450 \text{ pA}$; $V_{\text{bias}} = 965 \text{ mV}$; d) $I_t = 405 \text{ pA}$; $V_{\text{bias}} = 859 \text{ mV}$. The scale bar is 10nm.

Supporting Information

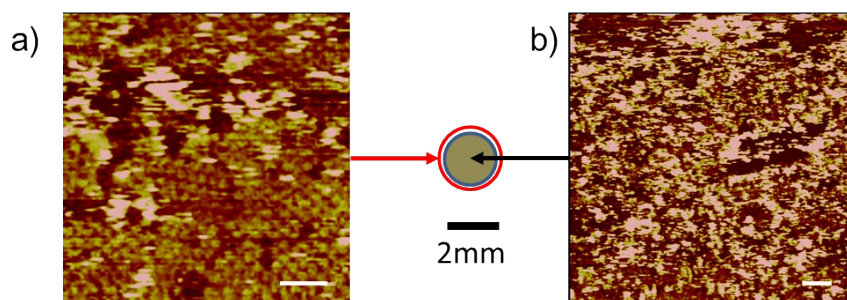


Figure S10. Relative positions of HHTP patterns after landing. STM image recorded at the center of the landing spot in a) showed orderly packed molecules; b) STM image at the center soft landing position showed no nanostructures but a scrambled surface with HHTP clusters. The center figure depicts the spatial separation of these images. Very far from the spot showed only plain HOPG substrate. The scale bar is 10nm for STM images.

Section 4. Simulation of HHTP interactions by DFT.

We inspected the interaction between two HHTP molecules and HHTP ions in the gas phase by DFT simulation using Gaussian 09. We consider the combination energy of three systems: HHTP/HHTP, HHTP/HHTP+H⁺ and HHTP+H⁺/HHTP+H⁺. Energy of molecules combining at different positions were calculated and the configurations of the three molecule pairs were optimized respectively. As to the neutral HHTP/HHTP, the geometry is that two molecules in two planes forming an acute angle with the lowest system energy (Figure S10a). The hydroxyl group in an adjacent benzene could form two strong hydrogen bonds in this geometry and the lengths of the two hydrogen bonds are both 1.85 Å. Regarding the charged HHTP molecules, the geometry at lowest energy is that one proton was shared by two oxygen atoms of different molecules, forming H-O...H⁺...O-H bonds (Figure 4b). However, the energy is higher than two separated HHTP+H⁺ ions. As to the combination of HHTP/HHTP+H⁺, neutral molecule and ion form a 'head to head' configuration. There are two hydrogen bonds and the proton was shared by the two molecules. The calculated energies reported as zero-point vibrational energy correction (ΔH_{0K}) of HHTP/HHTP is 0.58. ΔH_{0K} of proton HHTP+H⁺/HHTP+H⁺ is -0.19 and ΔH_{0K} of HHTP/HHTP⁺ is 1.28. The calculation results show that the combination of HHTP/HHTP or HHTP/HHTP+H⁺ is exothermic process, while it is an endothermic process for HHTP ions, thus unlikely happens. In the ambient SL process, the concentration of HHTP in each charged droplets is very low. Charged droplets prevent the clustering process of landed molecules because of the electric repulsion. After the species landed on HOPG, the molecules assemble to form a closely packed arrangement through Brownian motion and interactions with HOPG surface. The charge retained HHTP on surface may help to form the assembly with neutral molecules through the stronger bonding. The interaction between neutral HHTP and Na⁺ adducted HHTP is similar with the interaction between neutral HHTP and H⁺ adducted HHTP. Na-O interaction is weaker and we did not observe HHTP-Na-HHTP structures by STM. Thus the calculation of HHTP+Na⁺/HHTP was not mentioned here.

Supporting Information

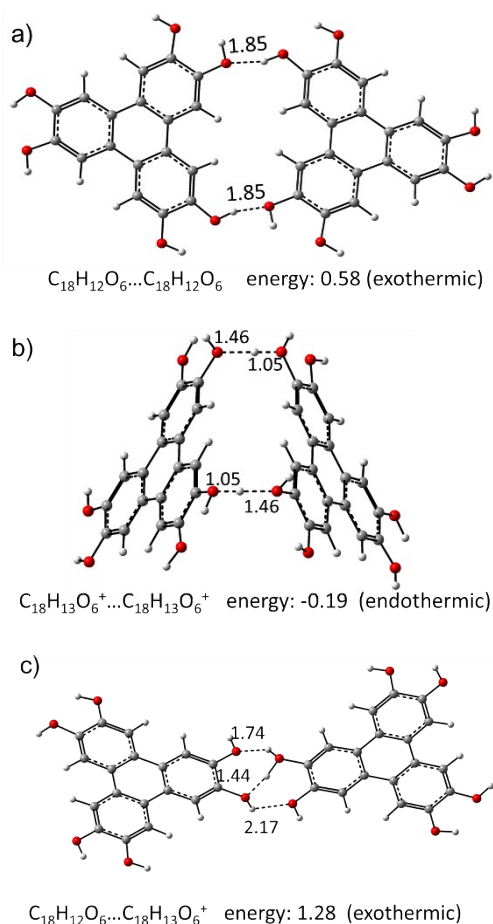


Figure S11. Optimized geometries of HHTP and HHTP+H⁺. The specific lowest energy geometry of HHTP/HHTP in a), HHTP⁺/HHTP⁺ in b) and HHTP/HHTP⁺ in c). The lengths of hydrogen bonds are given in the units of Å and the reported energy herein is zero-point vibrational energy correction (ΔH_{0K}).

Section 5. Analysis the deposited substances by ambient soft-landing

Before fabricating nanostructure on the HOPG, we collect the molecules on a silica substrate. The landed substances were rinsed off by 8 μ L methanol and water (1:1) except that BTB was rinsed off by methanol, water and THF (1:1:2). We analyzed the solution immediately using nanospray ionization in a Thermo LTQ linear ion trap mass spectrometry (Thermo Scientific, San Jose, CA, USA). Heat can have an effect on the spot area and ion current, but effect varies for different molecules. In SL, ion current increased from 0.6 nA to 3.0 nA under 100 °C for 5 mM C18H37NH2 with spot area increase to 8 mm in diameter. For 5mM C17H35COOH, heat has little effects on ion current.

Supporting Information

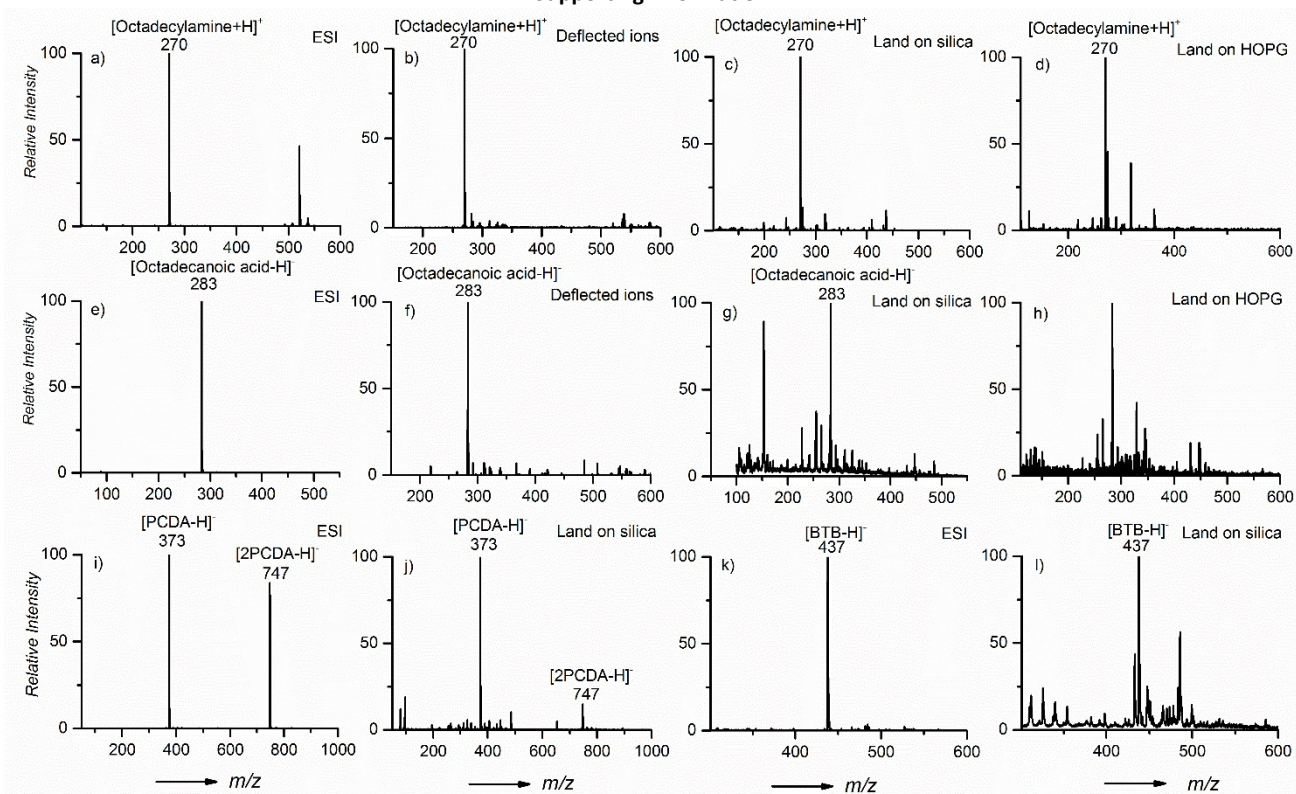


Figure S12. Mass spectra of substances before and after soft-landing process. a), e), i) and k) are the electrospray ionization mass spectra of 10^{-3} mol/L $C_{18}H_{37}NH_2$, $C_{17}H_{35}COOH$, PCDA dissolved in methanol and 10^{-3} mol/L BTB dissolved in methanol and THF (1:1), respectively. b) and f) represents the deflected $C_{18}H_{37}NH_2$ and $C_{17}H_{35}COOH$ ions into MS by apparatus in Figure 1b, respectively. c), g), j) and l) are mass spectra of collected $C_{18}H_{37}NH_2$, $C_{17}H_{35}COOH$, PCDA and BTB on silica by nanoESI, respectively. d) and h) are mass spectra of landed $C_{18}H_{37}NH_2$ and $C_{17}H_{35}COOH$ on HOPG. Mass spectra show that the molecules are intact after soft-landing process with little fragment.

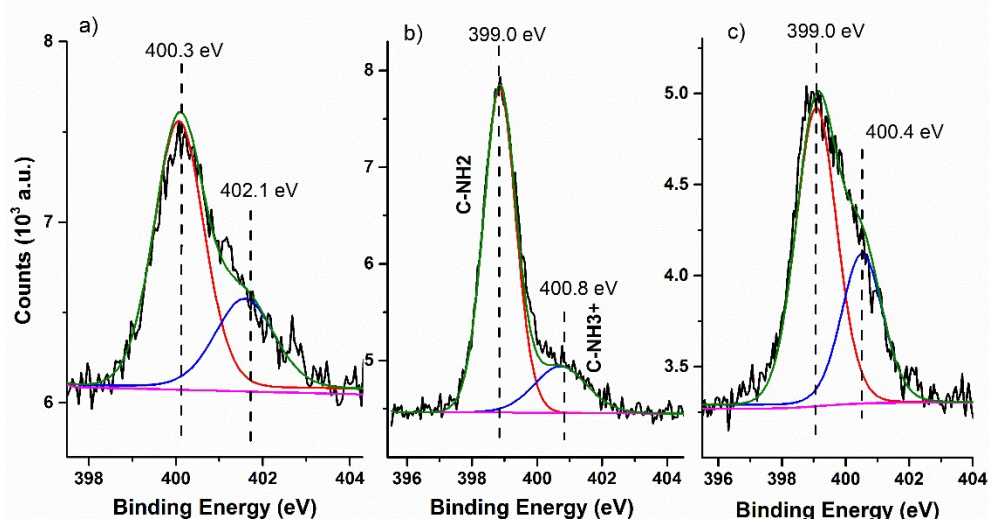


Figure S13. High resolution X-ray photoelectron spectra recorded for $C_{18}H_{37}NH_2$ by drop-casting a) and by soft-landing after 3 days b) and 14 days c) on HOPG, respectively. N 1s appears at 400.3 eV and 402.1 eV in a). High resolution X-ray photoelectron spectra recorded for n-octadecylamine landed on HOPG after b) 3 days and c) 14 days. N 1s appears at 399.0 eV and 400.8 eV in b), 399.0 eV and 400.4 eV in c), respectively. After 3 days, the peak 400.8 decreased compared to freshly prepared $C_{18}H_{37}NH_2$ (Figure 6), indicating the cations were

Supporting Information

neutralized by collision with gas ions in the air. After longer time like 14 days, the unstable species on surface changed.

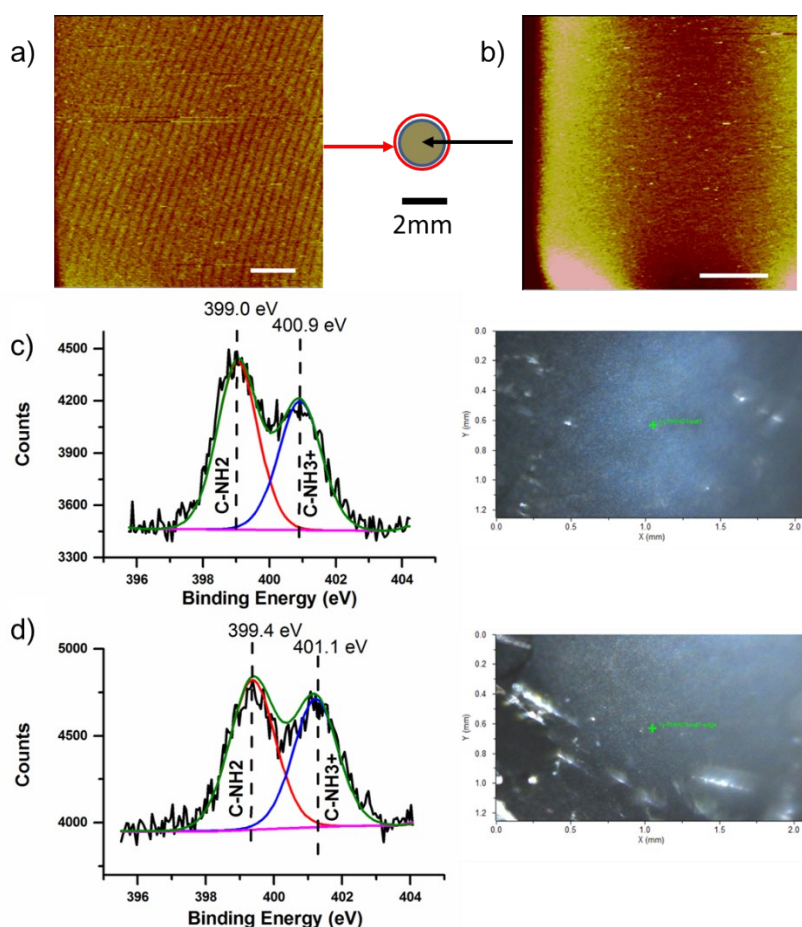


Figure S14. Relative positions of n-octadecylamine patterns after soft landing. STM image recorded (a) just outside the spot showed orderly packed molecules; (b) at the center soft landing position, STM image showed no nanostructures but HOPG substrate up and down. The center figure depicts the spatial separation of these images. Very far from the spot showed only plain HOPG substrate. The scale bar is 25nm. c) and d) are high resolution X-ray photoelectron spectra recorded for $C_{18}H_{37}NH_2$ species at the center of landing spot c) and at the periphery of the spot d) by SL with the drying tube heated to 100 °C. The binding energy both indicate $C_{18}H_{37}NH_2$ and $C_{18}H_{37}NH_3^+$ species on surface. Green crosses in the right photos point to the X-ray scanning sites, respectively. The scanning area of X- ray is 500*500 μm .

Section 6. The assembly of mixed n-octadecylamine and n-octadecanoic acid.

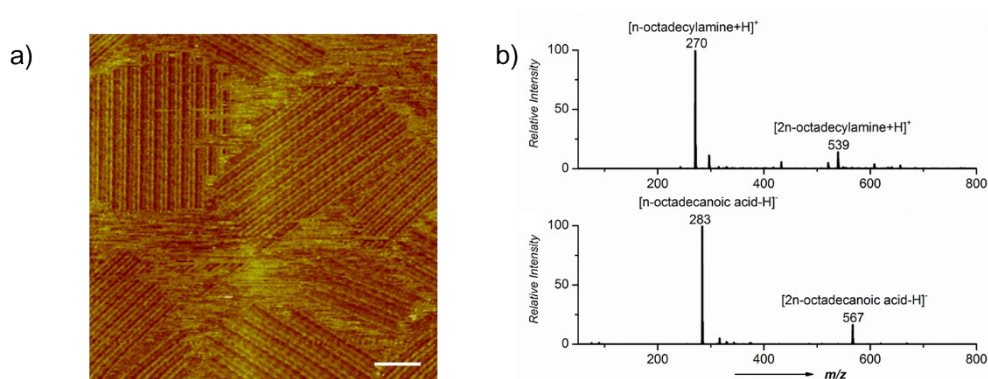


Figure S15. Results of mixed n-octadecylamine and n-octadecanoic acid. a) STM image of mixed n-octadecylamine and n-octadecanoic acid constructed by dropping 2.5 μL mixture solution on HOPG. The lattice parameters is $a = 6 \text{ nm}$, $b = 0.6 \text{ nm}$ and $\gamma = 90^\circ$. Image conditions: $I_t = 490 \text{ pA}$; $V_{\text{bias}} = 770 \text{ mV}$. The scale bar is 20 nm. We failed to find n-octadecylamine or n-octadecanoic acid to assembly by themselves in an appreciable area. b) The mass spectra of 1mmol/L mixed n-octadecylamine and n-octadecanoic acid by ESI in the positive mode and negative mode, respectively. We see the $\text{CH}_3(\text{CH}_2)_{17}\text{NH}_3^+$ (m/z 270) and its dimer (m/z 539) in a) without any sign of n-octadecanoic acid. In the negative mode, $\text{CH}_3(\text{CH}_2)_{17}\text{COO}^-$ (m/z 283) with its dimer (m/z 567) dominates the mass spectrum. The ESI has a selectivity for positive ions and negative ions.

References

- (1) Frisch, M. J.; Trucks, G. W.; Schlegel, H. B.; Scuseria, G. E.; Robb, M. A.; Cheeseman, J. R.; Scalmani, G.; Barone, V.; Mennucci, B.; Petersson, G. A.; Nakatsuji, H.; Caricato, M.; Li, X.; Hratchian, H. P.; Izmaylov, A. F.; Bloino, J.; Zheng, G.; Sonnenberg, J. L.; Hada, M.; Ehara, M.; Toyota, K.; Fukuda, R.; Hasegawa, J.; Ishida, M.; Nakajima, T.; Honda, Y.; Kitao, O.; Nakai, H.; Vreven, T.; Montgomery, J. A., Jr.; Peralta, J. E.; Ogliaro, F.; Bearpark, M.; Heyd, J. J.; Brothers, E.; Kudin, K. N.; Staroverov, V. N.; Kobayashi, R.; Normand, J.; Raghavachari, K.; Rendell, A.; Burant, J. C.; Iyengar, S. S.; Tomasi, J.; Cossi, M.; Rega, N.; Millam, J. M.; Klene, M.; Knox, J. E.; Cross, J. B.; Bakken, V.; Adamo, C.; Jaramillo, J.; Gomperts, R.; Stratmann, R. E.; Yazyev, O.; Austin, A. J.; Cammi, R.; Pomelli, C.; Ochterski, J. W.; Martin, R. L.; Morokuma, K.; Zakrzewski, V. G.; Voth, G. A.; Salvador, P.; Dannenberg, J. J.; Dapprich, S.; Daniels, A. D.; Farkas, O.; Foresman, J. B.; Ortiz, J. V.; Cioslowski, J.; Fox, D. J.; Gaussian 09, Revision A.1, Gaussian, Inc., Wallingford CT, 2009.
- (2) Becke, A.D. *J. Chem. Phys.* 1993, 98, 5648-5652.
- (3) Lee, C. T.; Yang, W. T.; Parr, R. G. *Phys. Rev. B* 1988, 37, 785-789.
- (4) Rassolov, V. A.; Pople, J. A.; Ratner, M. A.; Windus, T. L. *J. Chem. Phys.* 1998, 109, 1223-1229.